

Heavy hadron spectrum from 2+1+1 flavor MILC lattices

Sabiar Shaikh,^{a,*} Protick Mohanta,^b M. Padmanath^{b,c} and Subhasish Basak^{a,c}

^a*School of Physical Sciences, National Institute of Science Education and Research, An OCC of Homi Bhabha National Institute, Jatni 752050, India*

^b*The Institute of Mathematical Sciences, Chennai 600113, India*

^c*Homi Bhabha National Institute, Training School Complex, Anushakti Nagar, Mumbai 400094, India*

E-mail: sabiars@niser.ac.in, protickm@imsc.res.in, padmanath@imsc.res.in, sbasak@niser.ac.in

We study the mass spectra and various mass differences of heavy hadrons containing one or more bottom quarks using MILC's $N_f = 2 + 1 + 1$ HISQ gauge ensembles at three lattice spacings. For the valence quarks, we employ a combination of lattice actions: the NRQCD action is used for bottom quarks, the anisotropic Clover action for charm quarks, and the $O(a)$ -improved Wilson–Clover action for strange and lighter (up/down) quarks. Heavy hadron operators with at least one bottom quark are constructed by considering all possible combinations with charm, strange, and light quarks corresponding to various quantum numbers.

The 42nd International Symposium on Lattice Field Theory (LATTICE 2025)

2-8 November 2025

Tata Institute of Fundamental Research, Mumbai, India

*Speaker

1. Introduction

Lattice QCD has been extensively applied to B physics, especially for determining decay constants, mixing parameters, and meson mass differences relevant to CKM matrix elements [1]. Lattice QCD provides a first-principles approach to investigate the masses, splittings, and other properties of these baryons. Numerous studies have examined heavy baryons with one to three bottom quarks using various light quark actions [2–4]. The spectroscopy of heavy hadrons containing one or more bottom quarks provides a crucial window into the non-perturbative dynamics of QCD and tests lattice formulations for heavy quarks. Previous lattice studies have successfully used nonrelativistic QCD (NRQCD) to describe bottom quarks [5], yet achieving higher precision and controlling systematic uncertainties remain challenges, especially in light of ongoing experimental progress in heavy-flavor physics. In this work, we build on earlier investigations by simulating bottom quarks with NRQCD, charm quarks with an anisotropic clover action, and strange/light quarks with the Wilson–Clover action, enabling a systematic study of bottom-hadron spectroscopy with controlled discretization effects.

We present lattice QCD results for the ground-state spectra of hadrons containing at least one bottom quark, computed on MILC $N_f = 2 + 1 + 1$ HISQ ensembles at two lattice spacings, with a finer ensemble in progress. Interpolating operators are constructed for bottom mesons and baryons with all combinations of bottom, charm, strange, and light quarks. For baryons, we focus on positive-parity states with spins $J = \frac{1}{2}$ and $J = \frac{3}{2}$, and extract ground-state masses and mass differences. This study extends previous lattice work and represents a step toward precision determinations of bottom-hadron spectra from first principles, providing valuable input for current and future heavy-flavor experiments.

2. Quark action and tuning

2.1 NRQCD action for the bottom quark

In lattice QCD calculations of hadrons containing bottom quarks on relatively coarse lattices, NRQCD formulation is the most widely used approach [5]. The bottom quark inside a hadron is highly nonrelativistic, with $v^2 \sim 0.1$, as indicated by the comparison of bottomonium masses to the quark mass. For bottom hadrons with lighter valence quarks, the bottom quark velocity is even smaller, justifying the use of a nonrelativistic effective field theory. NRQCD thus provides a suitable framework for studying bottom quarks and is expected to remain the preferred method until finer lattices with $am_b < 1$ become widely available.

In NRQCD formulation, the upper and lower components of the Dirac spinor decouple and the bottom quark is described by two-component spinor fields. The NRQCD Lagrangian up to order $\mathcal{O}(v^4)$ is [6]

$$\mathcal{L} = \psi^\dagger (D_4 + H_0 + \delta H) \psi + \xi^\dagger (D_4 - \overline{H}_0 - \overline{\delta H}) \xi, \quad (1)$$

where ψ and ξ are the bottom quark and antiquark fields, respectively. The Hamiltonian H_0 contains the leading $\mathcal{O}(v^2)$ term and $\delta H = \sum \delta H_i$ contains the $\mathcal{O}(v^4)$ and $\mathcal{O}(v^6)$ terms with coefficients c_i . Similarly for \overline{H}_0 and $\overline{\delta H}$.

The various terms in the quark and antiquark Hamiltonians are [6, 7]

$$\begin{aligned}
H_0 &= -\frac{\Delta^2}{2m_b} = \overline{H_0} \\
\delta H_1 &= -c_1 \frac{(\Delta^2)^2}{8m_b^3} = \overline{\delta H_1} \\
\delta H_2 &= c_2 \frac{i}{8m_b^2} (\nabla \cdot \tilde{\mathbf{E}} - \tilde{\mathbf{E}} \cdot \nabla) = -\overline{\delta H_2} \\
\delta H_3 &= -c_3 \frac{1}{8m_b^2} \sigma \cdot (\tilde{\nabla} \times \tilde{\mathbf{E}} - \tilde{\mathbf{E}} \times \tilde{\nabla}) = -\overline{\delta H_3} \\
\delta H_4 &= -c_4 \frac{1}{2m_b} \sigma \cdot \tilde{\mathbf{B}} = \overline{\delta H_4} \\
\delta H_5 &= c_5 \frac{\Delta^4}{24m_b} = \overline{\delta H_5} \\
\delta H_6 &= -c_6 \frac{(\Delta^2)^2}{16nm_b^2} = \overline{\delta H_6}. \tag{2}
\end{aligned}$$

Here n is the factor in δH_6 to ensure numerical stability at small am_b with $n > 3/2m_b$ [8]. On the lattice, the heavy quark Green's function evolution is approximated by [5]

$$G_\psi(x, t+1; 0, 0) = \left(1 - \frac{\delta H}{2}\right) \left(1 - \frac{H_0}{2n}\right)^n U_t^\dagger(x, t) \left(1 - \frac{H_0}{2n}\right)^n \left(1 - \frac{\delta H}{2}\right) G_\psi(x, t; 0, 0), \tag{3}$$

with the initial condition

$$G_\psi(x, t; x_0, t_0) = \delta_{x, x_0} \delta_{t, t_0} \mathbb{I}. \tag{4}$$

The heavy-quark propagator G_ψ propagates only forward in time. Similarly, the heavy antiquark evolution equation with G_ξ evolving backwards in time is given by

$$G_\xi(x, t-1; 0, 0) = \left(1 - \frac{\overline{\delta H}}{2}\right) \left(1 - \frac{\overline{H_0}}{2n}\right)^n U_t(x, t-1) \left(1 - \frac{\overline{H_0}}{2n}\right)^n \left(1 - \frac{\overline{\delta H}}{2}\right) G_\xi(x, t; 0, 0), \tag{5}$$

using the initial condition

$$G_\xi(x, t; x_0, t_0) = -\delta_{x, x_0} \delta_{t, t_0} \mathbb{I}. \tag{6}$$

The open bottom system, B_s meson, is used for tuning the bottom quark. From the energy-momentum relation [7]

$$E(\mathbf{P}) = M_1 + \frac{\mathbf{P}^2}{2M_2}, \tag{7}$$

where M_1 is the pole mass, and the kinetic mass M_2 of B_s is tuned to match the PDG value of 5366.93 MeV. The hyperfine splitting, defined as

$$\Delta M_{B_s} = M_{B_s^*}^{\text{rest}} - M_{B_s}^{\text{rest}} = 48.5 \text{ MeV}, \tag{8}$$

provides a consistency check when using the pole masses of B_s and B_s^* at zero momentum. The NRQCD coefficients c_1, c_2, c_3, c_5, c_6 , the exponent n , and the tadpole factor u_0 are taken from HPQCD results [7]. The tuning parameters are the bare quark mass m_b and the coefficient c_4 . c_4 is the coefficient of order $O(1/m_b)$ term which gives the leading contribution in δH and control the hyperfine splitting.

2.2 Anisotropic clover action for charm quark

In this work, we use the anisotropic clover-improved Wilson action or Relativistic Heavy Quark (RHQ) action for the charm quark. The anisotropic Clover action modifies the standard Wilson-Clover formulation by introducing distinct spatial (a_s) and temporal (a_t) lattice spacings, leading to an anisotropy factor $\nu = a_s/a_t$. This setup enhances temporal resolution, which is crucial for heavy quark systems, while maintaining manageable lattice sizes. The RHQ action S_{RHQ} is given by [9, 10]

$$\begin{aligned} \frac{S_{\text{RHQ}}}{m_0 + 1 + 3\nu} &= \sum_n \bar{\psi}(n)\psi(n) - \kappa \left[\sum_n \bar{\psi}(n)(1 - \gamma_0)U_0(n)\psi(n + \hat{0}) \right. \\ &+ \sum_n \bar{\psi}(n)(1 + \gamma_0)U_0^\dagger(n - \hat{0})\psi(n - \hat{0}) + \nu \sum_{n,i} \bar{\psi}(n)(1 - \gamma_i)U_i(n)\psi(n + \hat{i}) \\ &\left. + \nu \sum_{n,i} \bar{\psi}(n)(1 + \gamma_i)U_i^\dagger(n - \hat{i})\psi(n - \hat{i}) \right] - \kappa c_P \sum_{n,\mu < \nu} \bar{\psi}(n)\sigma_{\mu\nu}F_{\mu\nu}(n)\psi(n), \quad (9) \end{aligned}$$

where $\kappa = \frac{1}{2(m_0 + 1 + 3\nu)}$, c_P is the clover coefficient, $\sigma_{\mu\nu} = \frac{i}{2}[\gamma_\mu, \gamma_\nu]$ is the antisymmetric tensor, and $F_{\mu\nu}(n)$ represents the discretized gluon field strength and taken to be hermitian. The determination of the RHQ action parameters $\{m_0, c_P, \nu\}$ is performed using the D_s meson correlations, as this choice mitigates both discretization effects and uncertainties from chiral extrapolation. The value of m_0 is tuned by matching lattice-calculated meson masses to experimental values. Specifically, the spin-averaged mass of the D_s and D_s^* mesons is used

$$\bar{M}_{D_s} = \frac{1}{4}M_{D_s} + \frac{3}{4}M_{D_s^*}. \quad (10)$$

The PDG value of \bar{M}_{D_s} is approximately 2.076 GeV. The clover coefficient c_P is adjusted so that the hyperfine splitting

$$\Delta M_{D_s} = M_{D_s^*} - M_{D_s}, \quad (11)$$

matches the PDG value of 143.8 MeV. The anisotropy coefficient ν is adjusted so that the meson dispersion relation satisfies the relativistic condition

$$E^2(\vec{p}) = M^2 + \vec{p}^2, \quad (12)$$

ensuring that the speed of light is correctly normalized on the lattice to $c^2 = 1$. We used $|\vec{p}| = \frac{2\pi}{L}$ in tuning the RHQ action parameters.

2.3 Clover action for strange, up/down quark

To simulate strange and light (up/down) quarks, we employ the $\mathcal{O}(a)$ -improved Wilson-Clover fermion action, which improves upon the original Wilson action by including a clover term that systematically removes leading discretization errors at $\mathcal{O}(a)$. The fermion action is expressed as

$$\begin{aligned} S_{\text{clover}} &= \sum_n \bar{\psi}(n)\psi(n) - \kappa_s \left[\sum_{n,\mu} \bar{\psi}(n)(1 - \gamma_\mu)U_\mu(n)\psi(n + \hat{\mu}) \right. \\ &\left. + \sum_{n,\mu} \bar{\psi}(n)(1 + \gamma_\mu)U_\mu^\dagger(n - \hat{\mu})\psi(n - \hat{\mu}) \right] - \kappa_s c_{\text{SW}} \sum_{n,\mu < \nu} \bar{\psi}(n)\sigma_{\mu\nu}F_{\mu\nu}(n)\psi(n) \quad (13) \end{aligned}$$

where $\kappa_s = \frac{1}{2(m+4)}$ and c_{SW} is the clover coefficient. In order to determine the κ_s , we have used the fictitious η_s meson. From chiral perturbation theory [8], its mass is estimated to be $m_{\eta_s} = 688.5$ MeV [11]. The bare quark mass is controlled via the hopping parameter κ_s , which is related to the bare mass through

$$ma = \frac{1}{2\kappa_s} - 4. \quad (14)$$

For light quarks (up/down), the hopping parameter $\kappa_{u/d}$ is tuned to obtain a lower pion mass m_π . The meson masses are extracted from two-point correlation functions computed on the lattice. Similarly, by tuning the values of κ_s , we set the η_s meson mass to be 688.5 MeV. The clover coefficient c_{SW} is tuned using the tadpole improvement prescription [12]

$$c_{\text{SW}} = \frac{1}{u_0^3}, \quad (15)$$

where u_0 is the tadpole improvement factor, typically defined via the fourth root of the average plaquette. This methodology provides a controlled and efficient framework for simulating strange and light quarks in lattice QCD using the improved Clover action.

3. Bottom baryon operators

To construct the baryon interpolating operators, we consider different quark compositions depending on the number of heavy quarks. For triple, double and single bottom baryons, the operators are defined in Table 1.

Baryon Type	Interpolating Operator
Triple-bottom	$(O_k^{hhh})_\alpha = \epsilon_{abc}(Q^{aT}C\gamma_k Q^b)Q_\alpha^c$
Double-bottom	$(O_k^{hh1})_\alpha = \epsilon_{abc}(Q^{aT}C\gamma_k Q^b)l_\alpha^c$
	$(O_k^{hlh})_\alpha = \epsilon_{abc}(Q^{aT}C\gamma_k l^b)Q_\alpha^c$
	$(O_5^{hlh})_\alpha = \epsilon_{abc}(Q^{aT}C\gamma_5 l^b)Q_\alpha^c$
Single-bottom	$(O_5^{hl_1l_2})_\alpha = \epsilon_{abc}(l_1^{aT}C\gamma_5 l_2^b)Q_\alpha^c$
	$(O_k^{hl_2l_1})_\alpha = \epsilon_{abc}(Q^{aT}C\gamma_k l_2^b)l_{1\alpha}^c$
	$(O_5^{hl_2l_1})_\alpha = \epsilon_{abc}(Q^{aT}C\gamma_5 l_2^b)l_{1\alpha}^c$

Table 1: Interpolating operators for bottom baryons.

Q denotes NRQCD bottom quarks [13], l is light or charm quarks, C is the charge-conjugation matrix, α is the spinor index, and

$$Q = \Theta(t-t') \begin{pmatrix} \psi_h \\ 0 \end{pmatrix} - \begin{pmatrix} 0 \\ \chi_h \end{pmatrix} \Theta(-t+t'). \quad (16)$$

Here, in the first term t' is positive, whereas in the second term t' is negative. These operators are constructed to respect color antisymmetry and the required spin structure, allowing for the extraction of ground-state baryon masses with different heavy-quark content.

4. Simulation Details

The simulations have been performed using three ensembles of MILC $N_f = 2 + 1 + 1$ HISQ lattices [7], the details of which are given in Table 2. The tuned parameters reported for $32^3 \times 96$ lattices are only for 50 configurations. The parameters are tuned for a smaller subset of configurations, and the production runs are ongoing. Here we present a status update of this ongoing effort. All measurements have been carried out using the point sources.

$\beta = 10/g^2$	am_l	am_s	am_c	$L^3 \times T$	a (fm)	N_{cfg}
5.80	0.013	0.065	0.838	$16^3 \times 48$	0.15	700
6.00	0.0102	0.0509	0.635	$24^3 \times 64$	0.12	700
6.30	0.0074	0.037	0.440	$32^3 \times 96$	0.09	50

Table 2: MILC configurations used in this work. The gauge coupling is β , lattice spacing a . am_l , am_s , and am_c are the light (up and down taken to have the same mass), strange and charm sea quark masses in lattice units, respectively, and the lattice size is $L^3 \times T$. The N_{cfg} is the number of configurations used in this work.

4.1 Strange quark tuning

For the strange-quark, the hopping parameter κ_s has been tuned separately for each lattice to get the ChiPT η_s mass as discussed above. The clover coefficient has been set to $c_{SW} = u_0^{-3}$ following Ref. [12], with the tadpole improvement factor u_0 taken from Ref. [14]. The resulting parameters are given in Table 3 for different lattices.

$L^3 \times T$	κ_s	c_{SW}
$16^3 \times 48$	0.14101	1.598
$24^3 \times 64$	0.140015	1.552
$32^3 \times 96$	0.138613	1.497

Table 3: Strange-quark hopping parameters and clover coefficients used in the simulations.

4.2 Charm-quark tuning

The charm-quark mass has been tuned for the RHQ action Eq. 9 by matching the spin-averaged D_s mass Eq. 10 and the hyperfine splitting Eq. 11 with the PDG values. The charm-quark tuning parameters are given in Table 4.

$L^3 \times T$	m_0	c_P	ν	\bar{M}_{D_s} (MeV)	ΔM_{D_s} (MeV)	c^2
$16^3 \times 48$	0.6647	2.5822	1.2488	2076 (9)	144 (9)	1.0003
$24^3 \times 64$	0.2033	1.9264	1.2168	2076 (7)	144 (7)	0.9999
$32^3 \times 96$	-0.556	0.36	1.52	2077 (15)	144 (15)	1.0028
PDG				2076.24	143.8	

Table 4: Charm-quark tuning using the \bar{M}_{D_s} and ΔM_{D_s} .

4.3 Bottom-quark tuning

The bottom-quark mass has been tuned for the NRQCD action Eq. 1 by matching the kinetic mass of the B_s Eq. 7 and the hyperfine splitting ΔM_{B_s} Eq. 8 with the PDG values. The bottom-quark tuning parameters are given in Table 5.

$L^3 \times T$	m_b	c_4	B_s kinetic mass (MeV)	ΔM_{B_s} (MeV)
$16^3 \times 48$	3.8167	1.4456	5367	48.5
$24^3 \times 64$	2.2498	1.0336	5367	48.5
$32^3 \times 96$	1.44	0.9	5366	49.1
PDG			5366.93	48.5

Table 5: Bottom-quark tuning using the B_s kinetic mass and ΔM_{B_s} . The error in determining kinetic mass is around 2.5%.

In the NRQCD formulation, absolute hadron masses are not directly accessible due to the omission of the heavy quark mass term from the action. The physical B_s meson mass is reconstructed by adding an ensemble-dependent energy offset to the pole mass extracted from the two-point correlation functions. The kinetic masses reproduce the experimental B_s mass, while the offsets account for the missing rest-mass contribution in NRQCD.

5. Results and Discussions

Unitarity of the four-component NRQCD formulation was investigated by comparing effective masses extracted from correlation functions of forward and backward propagation of η_b . Within statistical uncertainties, the effective masses obtained from the forward and backward propagations are found to agree over the plateau region, resulting in a consistent ground-state extraction, indicating unitarity is preserved in the four-component NRQCD approach. The resulting plots are shown in Fig. 1 for η_b .

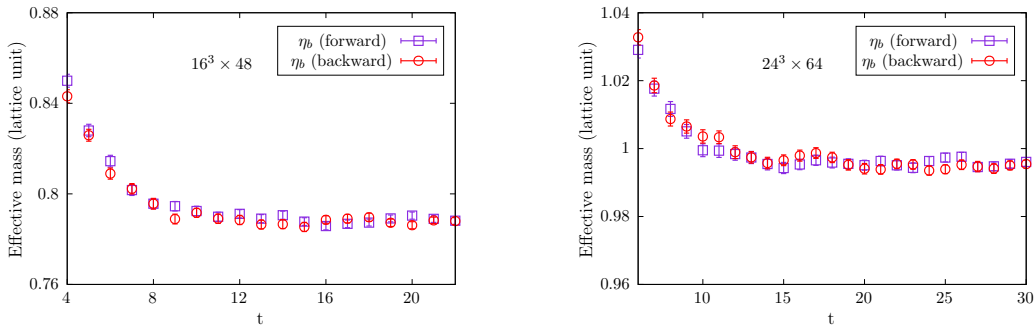


Figure 1: Effective masses of forward and backward propagation of η_b , on $16^3 \times 48$ and $24^3 \times 64$ lattices, obtained for test of unitarity.

The B_c meson, which contains both a bottom and a charm quark, provides a stringent test of the simultaneous tuning of the NRQCD action for the bottom quark and the RHQ action for the charm quark. We compute the B_c two-point correlation functions on the $16^3 \times 48$ and $24^3 \times 64$ ensembles

and extract the corresponding effective masses. The resulting effective mass plots exhibit clear and stable plateaus over an extended range of Euclidean time. This enables us to reliably extract the ground-state. A representative effective-mass results for the two ensembles are shown in Fig. 2.

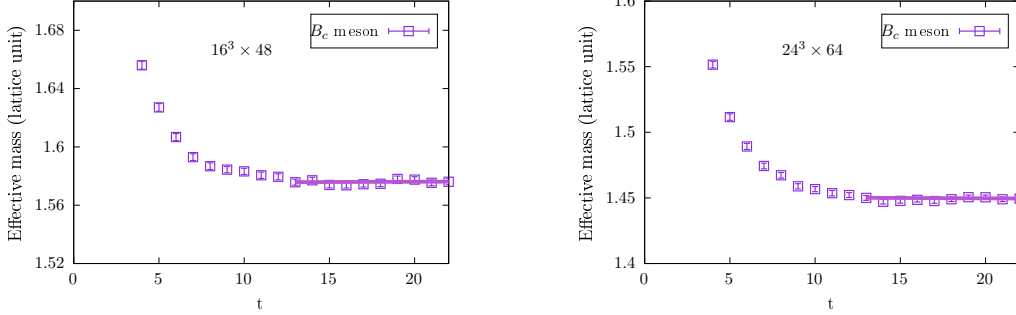


Figure 2: Effective mass plots for B_c . The bands are placed over the fit range.

We extract baryon masses from two-point correlation functions on the $16^3 \times 48$ and $24^3 \times 64$ ensembles. The corresponding effective masses exhibit reasonably long plateaus over Euclidean time. A representative effective-mass plots for the two ensembles are shown in Fig. 3, demonstrating stable and consistent behavior across the plateau region.

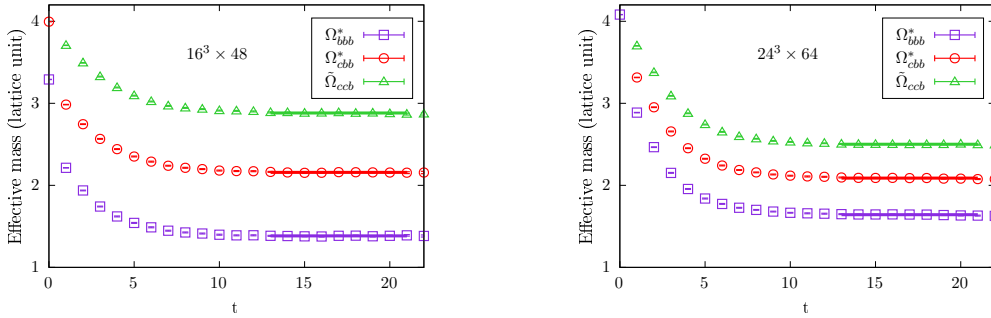


Figure 3: Ω_{bbb}^* , Ω_{cbb}^* , and $\tilde{\Omega}_{ccb}$ effective masses for $16^3 \times 48$ and $24^3 \times 64$ ensembles.

The resulting baryon mass spectra was computed on the $16^3 \times 48$ and $24^3 \times 64$ ensembles. As shown in Fig. 4, our results for both single and multiple-bottom baryons are in good agreement with previous lattice calculations, demonstrating the consistency and reliability of our heavy-quark tuning and methodology. The spectra exhibits the expected mass hierarchies and splittings, providing a comprehensive benchmark for future comparisons with experimental and lattice data.

6. Summary and Outlook

In this talk, we give a status update of the lattice QCD study of heavy hadron mass spectra containing one or more bottom quarks using 2 + 1 + 1 flavor HISQ ensembles generated by the MILC Collaboration. Our calculations have been performed at two lattice spacings, with a third finer lattice spacing currently in progress, to get continuum extrapolation and improved control over discretization effects. A mixed-action approach is employed, using NRQCD for bottom quarks,

RHQ action for charm quarks, and the clover-improved Wilson action for strange and light quarks. The quark masses are tuned carefully using known hadron masses, including η_s , D_s , and B_s , to ensure accurate reproduction of physical observables.

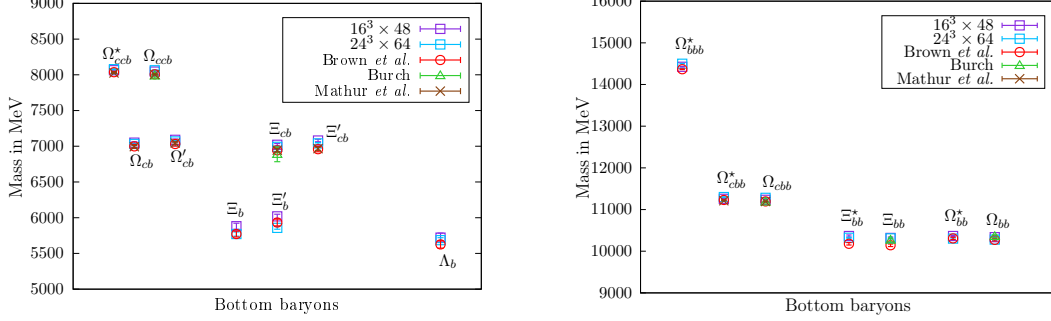


Figure 4: Comparison of our single, double and triple bottom baryon spectra with Brown et al. [4], Burch [15], and Mathur et al. [2, 16].

Our analysis focuses primarily on the ground-state masses of single and multiple-bottom hadrons. The resulting spectra exhibit stable effective-mass plateaus and show good agreement with available experimental values and previous lattice calculations. This consistency confirms the reliability of our mixed-action setup for heavy-quark physics. Future work will extend these studies to hyperfine splittings, mass differences, and additional heavy-baryon states. These investigations will lead to a more complete understanding of the heavy-hadron spectrum. They will also provide important benchmarks for both experimental measurements and theoretical models.

Acknowledgement

We acknowledge financial support from the Department of Atomic Energy (DAE), Government of India, and NISER, Bhubaneswar. We thank the MILC Collaboration for providing the HISQ gauge ensembles used in this work. Simulations have been carried out on the Bihan cluster of the School of Physical Sciences, NISER and the Kamet cluster at IISc. MP gratefully acknowledges support from the Department of Science and Technology, India, SERB Start-up Research Grant No. SRG/2023/001235. We also thank Srijit Paul for helping with the HISQ gauge configurations.

References

- [1] C. Davies, PoS **LATTICE2011**, 019 (2011) doi:10.22323/1.139.0019 [arXiv:1203.3862 [hep-lat]].
- [2] N. Mathur, M. Padmanath and S. Mondal, Phys. Rev. Lett. **121**, no.20, 202002 (2018) doi:10.1103/PhysRevLett.121.202002 [arXiv:1806.04151 [hep-lat]].
- [3] S. Meinel, Phys. Rev. D **82**, 114514 (2010) doi:10.1103/PhysRevD.82.114514 [arXiv:1008.3154 [hep-lat]].

- [4] Z. S. Brown, W. Detmold, S. Meinel and K. Orginos, Phys. Rev. D **90**, no.9, 094507 (2014) doi:10.1103/PhysRevD.90.094507 [arXiv:1409.0497 [hep-lat]].
- [5] G. P. Lepage, L. Magnea, C. Nakhleh, U. Magnea and K. Hornbostel, Phys. Rev. D **46**, 4052-4067 (1992) doi:10.1103/PhysRevD.46.4052 [arXiv:hep-lat/9205007 [hep-lat]].
- [6] G. T. Bodwin, E. Braaten and G. P. Lepage, Phys. Rev. D **51**, 1125-1171 (1995) [erratum: Phys. Rev. D **55**, 5853 (1997)] doi:10.1103/PhysRevD.55.5853 [arXiv:hep-ph/9407339 [hep-ph]].
- [7] R. J. Dowdall *et al.* [HPQCD], Phys. Rev. D **85**, 054509 (2012) doi:10.1103/PhysRevD.85.054509 [arXiv:1110.6887 [hep-lat]].
- [8] P. Mohanta and S. Basak, Phys. Rev. D **101**, no.9, 094503 (2020) doi:10.1103/PhysRevD.101.094503 [arXiv:1911.03741 [hep-lat]].
- [9] N. H. Christ, M. Li and H. W. Lin, Phys. Rev. D **76**, 074505 (2007) doi:10.1103/PhysRevD.76.074505 [arXiv:hep-lat/0608006 [hep-lat]].
- [10] Y. Aoki *et al.* [RBC and UKQCD], Phys. Rev. D **86**, 116003 (2012) doi:10.1103/PhysRevD.86.116003 [arXiv:1206.2554 [hep-lat]].
- [11] R. J. Dowdall, C. T. H. Davies, G. P. Lepage and C. McNeile, Phys. Rev. D **88**, 074504 (2013) doi:10.1103/PhysRevD.88.074504 [arXiv:1303.1670 [hep-lat]].
- [12] A. Bazavov *et al.* [Fermilab Lattice and MILC], Phys. Rev. D **85**, 114506 (2012) doi:10.1103/PhysRevD.85.114506 [arXiv:1112.3051 [hep-lat]].
- [13] L. Leskovec, S. Meinel, M. Pflaumer and M. Wagner, Phys. Rev. D **100**, no.1, 014503 (2019) doi:10.1103/PhysRevD.100.014503 [arXiv:1904.04197 [hep-lat]].
- [14] A. Bazavov *et al.* [MILC], Phys. Rev. D **82**, 074501 (2010) doi:10.1103/PhysRevD.82.074501 [arXiv:1004.0342 [hep-lat]].
- [15] T. Burch, [arXiv:1502.00675 [hep-lat]].
- [16] N. Mathur, R. Lewis and R. M. Woloshyn, Phys. Rev. D **66**, 014502 (2002) doi:10.1103/PhysRevD.66.014502 [arXiv:hep-ph/0203253 [hep-ph]].